Coupling of Discontinuous and Continuous Finite Element Methods for Environmental Quality Modeling Applications

Clint Dawson and Jennifer Proft
Center for Subsurface Modeling
Texas Institute for Computational and Applied Mathematics
University of Texas, Austin, TX 78712

Abstract

In this paper, we formulate a coupled discontinuous/continuous Galerkin method for the numerical solution of convection-diffusion type equations which arise in environmental quality modeling. One motivation for this approach is to use a discontinuous method where the solution is rough, e.g., in regions of high gradients, and use a continuous method where the solution is smooth. In this approach, the domain is decomposed into two regions, and appropriate transmission conditions are applied at the interface between regions. In one region, a local discontinuous Galerkin method is applied, and in the other region a standard continuous Galerkin method is employed.

Introduction

Galerkin finite element methods, with continuous, piecewise polynomial approximating spaces, have long been employed to approximate solutions to partial differential equations. Within the past few years, however, a number of researchers have investigated Galerkin methods based on fully discontinuous approximating spaces, the so-called discontinuous Galerkin (DG) methods [10].

DG methods possess several interesting features which may be useful in certain applications. First, they easily allow for varying the polynomial order of approximation from one element to the next. They allow for very general meshes, including nonconforming meshes, without hanging nodes or the need for a mortar space. One can also build stability post-processing into the methods for minimizing oscillations in the presence of high gradients. Finally, the methods are "locally conservative," that is, they are based on satisfying conservation principles element-by-element. One potential disadvantage of DG methods over continuous Galerkin methods is that the degrees of freedom in a DG method are associated with elements, while in the continuous Galerkin method they are associated with nodes. Hence, for the same degree

approximating spaces on the same grid, there may be many more degrees of freedom needed for the DG method. Even in a one-dimensional mesh with N elements, there are $N+1$ degrees of freedom when using a continuous, piecewise linear space, and $2N$ degrees of freedom when using a discontinuous, piecewise linear space.

Recently, the authors and collaborators have investigated a variant of the DG method, known as the local discontinuous Galerkin (LDG) method, for convection-diffusion equations. The LDG method was first proposed by Bassi and Rebay [4] for the Navier-Stokes equations, and first analyzed by Cockburn and Shu [12]. Cockburn and Dawson extended this analysis to variable coefficient, multidimensional transport problems with more general boundary conditions [7], and in collaboration with Aizinger and Castillo, studied the method for the solution of contaminant transport problems [2]. Recently, Aizinger and Dawson also applied the LDG method to the shallow water equations [1]. LDG methods have been studied for elliptic equations [5, 8], electromagnetics [3] and Stokes problems [9].

In environmental quality modeling, such as contaminant transport and circulation in shallow water systems, there are often regions where the solution is "smooth" transitioning to regions where the solution is "rough." In the smooth regions, it may be advantageous to use continuous Galerkin methods, which are well-known to give good approximations to smooth solutions. Where the solution is rough, it may be better to use a DG method, since these methods have built-in stabilizing mechanisms (e.g. slope limiting). Another reason for using a DG method in parts of the domain is to utilize their ability to easily incorporate h and p adaptivity. In this paper, we propose a coupled continuous-discontinuous Galerkin approach. We study such an approach for linear transport problems, such as those arising in contaminant transport, and develop appropriate transmission conditions across interfaces between the two methods. In future research, we hope to apply this idea to the numerical simulation of shallow water hydrodynamics and other transport type applications.

A coupled continuous-discontinuous approach has also been studied by Perugia and Schötzau [15] for the modeling of elliptic problems arising in electromagnetics. The motivation for their work was the ability of the DG method to handle nonmatching element interfaces. This feature is of interest in our applications, but we are also concerned with the DG method's ability to handle transient flow with sharp fronts.

The paper is organized as follows. In the next section, we state the problem to be considered and formulate the coupled LDG-continuous Galerkin finite element (CFE) method. Then, in section three, some numerical results are given.

Problem definition and coupled LDG/CFE method

Let Ω be a bounded domain in $\mathbb{R}^d$, $d = 1, 2$ or 3, with boundary $\partial\Omega$ decomposed into inflow $\partial\Omega_i$ and outflow/noflow $\partial\Omega_o$ portions

$$\partial\Omega_i = \{x \in \partial\Omega : u \cdot n < 0\}, \tag{1}$$
$$\partial\Omega_o = \{x \in \partial\Omega : u \cdot n \geq 0\}, \tag{2}$$

determined by a given velocity field u, where n is the unit outward normal to $\partial\Omega$.

Consider the model transport problem: find $c = c(x,t)$ such that

$$\partial_t c + \nabla \cdot (uc - D\nabla c) + \alpha c = f, \qquad (x,t) \in \Omega,\ t > 0, \tag{3}$$
$$(uc - D\nabla c) \cdot n = (u \cdot n)g, \qquad \text{on } \partial\Omega_i, \tag{4}$$
$$(-D\nabla c) \cdot n = 0, \qquad \text{on } \partial\Omega_o. \tag{5}$$
$$c(x,0) = c^0(x), \qquad \text{on } \Omega. \tag{6}$$

Here g and c^0 are specified boundary and initial data respectively; $\alpha \geq 0$ and D is assumed to be symmetric, positive semi-definite and bounded. We assume the coefficients, initial and boundary data, and domain are sufficiently smooth so that a unique solution c exists.

Let $\{\mathcal{T}_h\}_{h>0}$ denote a quasi-uniform family of finite element partitions of Ω such that no element Ω_e crosses $\partial\Omega$. Let h_e denote the element diameter and h the maximal element diameter. We assume each element Ω_e has a Lipschitz boundary $\partial\Omega_e$.

For any function $w \in H^1(\Omega_e)$ for each element Ω_e, we denote its trace on $\partial\Omega_e$ from inside Ω_e by w^i, and (when appropriate) the trace from outside Ω_e by w^o. Let n_i denote a fixed unit vector normal to any interior face γ_i between elements. Set

$$w^-(\mathbf{x}) = \lim_{s \to 0-} w(\mathbf{x} + sn_i), \qquad w^+(\mathbf{x}) = \lim_{s \to 0+} w(\mathbf{x} + sn_i),$$

then define

$$\overline{w} = \frac{1}{2}(w^+ + w^-), \qquad [w] = w^- - w^+.$$

Consider a partition of domain Ω into two disjoint subdomains Ω_I and Ω_{II} with interface Γ internal to Ω. Let c_I denote the restriction of c to Ω_I, and c_{II} the restriction of c to Ω_{II}. We will define our coupled method by discretizing the problem in Ω_I via the LDG Method and in Ω_{II} via the standard Galerkin finite element method. We assume that element boundaries in the triangulation $\mathcal{T}_h$ align with the interface Γ. In Ω_I, because of the flexibility of the LDG method, we can allow for the elements Ω_e

to be nonconforming; that is, the element boundaries need not match. However, we will assume that any face γ in the mesh intersects at most N elements, where N is bounded independent of h.

Weak formulations

In Ω_I, we rewrite (3) in a mixed form

$$\partial_t c_I + \nabla(uc_I + z) + \alpha c_I = f, \tag{7}$$

$$\tilde{z} = -\nabla c_I, \tag{8}$$

$$z = D\tilde{z}. \tag{9}$$

with boundary conditions

$$\begin{aligned} (uc_I + z)\cdot n &= (u\cdot n)g \quad \text{on } \partial\Omega_I \cap \partial\Omega_i, & (10)\\ z\cdot n &= 0 \qquad\quad \text{on } \partial\Omega_I \cap \partial\Omega_o. & (11) \end{aligned}$$

We will use the $L^2(R)$ inner product notation $(\cdot,\cdot)_R$ for domains $R \in I\!R^d$, and the notation $\langle u, v\rangle_R$ to denote integration over $d-1$ dimensional surfaces. Multiply the above equations by arbitrary, smooth test functions $w \in H^1(\Omega_e)$, v, $\tilde{v} \in (H^1(\Omega_e))^d$ respectively, and integrate by parts over each element $\Omega_e \subset \Omega_I$ to obtain

$$\begin{aligned} &(\partial_t c_I, w)_{\Omega_e} - (u\,c_I + z, \nabla w)_{\Omega_e} + \langle (u\,c_I + z)\cdot n_e, w\rangle_{\partial\Omega_e/\partial\Omega_I} \\ &+\langle u\,c_I\cdot n, w\rangle_{\partial\Omega_e\cap\partial\Omega_o} + \langle (u\,c_I + z)\cdot n, w\rangle_{\partial\Omega_e\cap\Gamma} + (\alpha c_I, w)_{\Omega_e} \\ &\qquad = (f,w)_{\Omega_e} - \langle (u\cdot n)g, w\rangle_{\partial\Omega_e\cap\partial\Omega_i}, \end{aligned} \tag{12}$$

$$(\tilde{z}, v)_{\Omega_e} - (c_I, \nabla\cdot v)_{\Omega_e} + \langle c_I, v\cdot n_e\rangle_{\partial\Omega_e} = 0, \tag{13}$$

and

$$(D\tilde{z}, \tilde{v})_{\Omega_e} - (z, \tilde{v})_{\Omega_e} = 0. \tag{14}$$

In Ω_{II}, we apply the continuous Galerkin finite element method. The weak form is obtained by multiplying (3) by $r \in H^1(\Omega_{II})$ and integrating by parts over the subdomain to obtain

$$\begin{aligned} &(\partial_t c_{II}, r)_{\Omega_{II}} - (u\,c_{II} - D\nabla c_{II}, \nabla r)_{\Omega_{II}} + \langle u\,c_{II}\cdot n, r\rangle_{\partial\Omega_{II}\cap\partial\Omega_o} \\ &+\langle (u\,c_{II} - D\nabla c_{II})\cdot n, r\rangle_{\Gamma} + (\alpha c_{II}, r)_{\Omega_{II}} \\ &\qquad = (f,r)_{\Omega_{II}} - \langle (u\cdot n)g, r\rangle_{\partial\Omega_{II}\cap\partial\Omega_i} \end{aligned} \tag{15}$$

On the interface Γ, fix the unit normal n_Γ to face outward from Ω_I and inward to Ω_{II}. We require the following transmissibility conditions between the two domains:

$$c_I = c_{II} \quad \text{at } \Gamma, \tag{16}$$

$$D\nabla c_I \cdot n_\Gamma = D\nabla c_{II} \cdot n_\Gamma \quad \text{at } \Gamma. \tag{17}$$

Coupling the LDG to the CFE method

In this section we formulate the coupling of the LDG method discretizing Ω_I and the continuous Galerkin method discretizing Ω_{II}. On $\Omega_e \subset \Omega_I$, we use the approximating space $\mathcal{P}^{k_e}(\Omega_e)$, where $\mathcal{P}^{k_e}$ denotes the set of polynomials of degree at most k_e. Let

$$W_h = \{w : \Omega_I \to I\!R : w|_{\Omega_e} \in \mathcal{P}^{k_e}(\Omega_e)\}.$$

On Ω_{II}, we use the approximating space $R_h \subset H^1(\Omega_{II})$ consisting of continuous, piecewise polynomials of degree at most k.

In Ω_I, we approximate $c_I(\cdot,t)$ by $C_I(\cdot,t) \in W_h$, $z(\cdot,t)$ by $Z(\cdot,t) \in (W_h)^d$, and $\tilde{z}(\cdot,t)$ by $\tilde{Z}(\cdot,t) \in (W_h)^d$, where C_I, Z and $\tilde{Z}$ satisfy weak formulations similar to (12)-(14). In (12) the values of c_I and z across element boundaries are approximated by

$$c_I \approx C_I^u = \begin{cases} C_I^i, & u \cdot n_e > 0, \\ C_I^o, & u \cdot n_e \le 0, \end{cases} \quad \text{on } \partial\Omega_e/\partial\Omega_I,$$

$$z \approx \overline{Z}, \quad \text{on } \partial\Omega_e/\partial\Omega_I.$$

In (13) the value of c_I across element boundaries is defined as:

$$c_I \approx \bar{C}_I \quad \text{on } \partial\Omega_e/\partial\Omega_I. \tag{18}$$

We define transmissibility conditions for c and z at the interface to be:

$$c \approx C_\Gamma^u = \begin{cases} C_I, & u \cdot n_\Gamma > 0, \\ C_{II}, & u \cdot n_\Gamma < 0, \end{cases} \quad \text{at } \Gamma \text{ in equations (12) and (15)}, \tag{19}$$

$$z = -D\nabla c \approx Z \quad \text{at } \Gamma \text{ in equations (12) and (15)}, \tag{20}$$

$$c \approx C_{II} \quad \text{at } \Gamma \text{ in equation (13)}, \tag{21}$$

Incorporating these boundary conditions, edge, and interface approximations, we sum (12), (13) and (14) over all elements $\Omega_e \in \Omega_I$. Let $\sum_e$ denote summation over all

elements $\Omega_e \subset \Omega_I$, and let $\sum_i$ denote summation over all interior boundaries γ_i such that $\gamma_i \notin \Gamma$ of domain Ω_I. Consider the following functionals:

$$\begin{aligned}\mathcal{A}(C_I, C_\Gamma^u, Z, w) &= \sum_e [(\partial_t C_I, w)_{\Omega_e} - (uC_I + Z, \nabla w)_{\Omega_e} + (\alpha C_I, w)_{\Omega_e}] \\ &+ \sum_i \langle (uC_I^u + \overline{Z}) \cdot n_i, [w] \rangle_{\gamma_i} + \langle (uC_I) \cdot n, w \rangle_{\partial\Omega_I \cap \partial\Omega_o} \\ &+ \langle (uC_\Gamma^u + Z) \cdot n_\Gamma, w \rangle_\Gamma,\end{aligned} \tag{22}$$

$$\begin{aligned}\mathcal{B}(C_I, C_{II}, \tilde{Z}, v) &= \sum_e [(\tilde{Z}, v)_{\Omega_e} - (C_I, \nabla \cdot v)_{\Omega_e}] + \sum_i \langle \bar{C}_I, [v] \cdot n_i \rangle_{\gamma_i} \\ &+ \langle C_I, v \cdot n \rangle_{\partial\Omega_I/\Gamma} + \langle C_{II}, v \cdot n_\Gamma \rangle_\Gamma,\end{aligned} \tag{23}$$

$$\mathcal{C}(Z, \tilde{Z}, \tilde{v}) = \sum_e [(-Z, \tilde{v})_{\Omega_e} + (D\tilde{Z}, \tilde{v})_{\Omega_e}], \tag{24}$$

$$\begin{aligned}\mathcal{D}(C_{II}, C_\Gamma^u, Z, r) &= (\partial_t C_{II}, r)_{\Omega_{II}} - (u\, C_{II}, \nabla r)_{\Omega_{II}} + (D\nabla C_{II}, \nabla r)_{\Omega_{II}} \\ &+ (\alpha C_{II}, r)_{\Omega_{II}} + \langle (u\, C_{II}) \cdot n, r \rangle_{\partial\Omega_{II} \cap \partial\Omega_o} \\ &- \langle u\, C_\Gamma^u \cdot n_\Gamma, r \rangle_\Gamma - \langle Z \cdot n_\Gamma, r \rangle_\Gamma.\end{aligned}$$

$$\mathcal{L}(w) = \sum_e (f, w)_{\Omega_e} + \langle gu \cdot n, w \rangle_{\partial\Omega_I \cap \partial\Omega_i}, \tag{25}$$

$$\mathcal{F}(r) = (f, r)_{\Omega_{II}} - \langle gu \cdot n, r \rangle_{\partial\Omega_{II} \cap \partial\Omega_i}. \tag{26}$$

We are now prepared to formulate the coupled LDG and CFE method. At t=0 we define $C_I(\cdot, 0) \equiv C_I^0 \in W_h$, and $C_{II}(\cdot, 0) \equiv C_{II}^0 \in R_h$ by

$$(C_I^0 - c_I^0, w)_{\Omega_I} = 0, \quad \forall\, w \in W_h, \tag{27}$$

$$(C_{II}^0 - c_{II}^0, r)_{\Omega_{II}} = 0, \quad \forall\, r \in R_h). \tag{28}$$

For each $t > 0$, we seek $(C_I, C_{II}, Z, \tilde{Z}) \in W_h \times R_h \times (W_h)^d \times (W_h)^d$ satisfying

$$\mathcal{A}(C_I, C_\Gamma^u, Z, w) = \mathcal{L}(w) \quad \forall\, w \in W_h, \tag{29}$$

$$\mathcal{B}(C_I, C_{II}, \tilde{Z}, v) = 0 \quad \forall\, v \in (W_h)^d, \tag{30}$$

$$\mathcal{C}(Z, \tilde{Z}, \tilde{v}) = 0 \quad \forall\, \tilde{v} \in (W_h)^d, \tag{31}$$

$$\mathcal{D}(C_{II}, C_\Gamma^u, Z, r) = \mathcal{F}(r) \quad \forall\, r \in R_h. \tag{32}$$

In [13], the following stability and error estimate are proven for the method outlined above.

Proposition 1 *The scheme (27)-(32) satisfies the stability result*

$$|\!|\!| (C_I, C_{II}, \tilde{Z}) |\!|\!| \leq (||c^0||^2_\Omega + \int_0^T \langle |u \cdot n|, g^2 \rangle_{\partial\Omega_i} dt)^{1/2} + \int_0^T ||f||_\Omega \, dt.$$

where

$$\begin{aligned} |\!|\!| (C_I, C_{II}, \tilde{Z}) |\!|\!|^2 &= ||C_I(T)||^2_{\Omega_I} + ||C_{II}(T)||^2_{\Omega_{II}} \\ &+ 2\int_0^T ||\alpha^{1/2} C_I||^2_{\Omega_I} dt + 2\int_0^T ||\alpha^{1/2} C_{II}||^2_{\Omega_{II}} dt \\ &+ 2\int_0^T ||D^{1/2}\tilde{Z}||^2_{\Omega_I} dt + 2\int_0^T ||D^{1/2}\nabla C_{II}||^2_{\Omega_{II}} dt \\ &+ \int_0^T \sum_i \langle |u \cdot n_i|, [C_I]^2 \rangle_{\gamma_i} dt + \int_0^T \langle |u \cdot n_\Gamma|, (C_I - C_{II})^2 \rangle_\Gamma dt \\ &+ \int_0^T \langle |u \cdot n|, (C_{II})^2 \rangle_{\partial\Omega_{II} \cap \partial\Omega_o} dt + \int_0^T \langle |u \cdot n|, (C_I)^2 \rangle_{\partial\Omega_I \cap \partial\Omega_o} \, dt. \end{aligned}$$

Theorem 1 *For c sufficiently smooth and $u \in W^1_\infty(\Omega)$, the scheme (27)-(32) satisfies the error estimate*

$$|\!|\!| (c_I - C_I, c_{II} - C_{II}, \tilde{z} - \tilde{Z}) |\!|\!| \leq K h^k,$$

where k is the minimal degree of polynomial used to define W_h and R_h, and K is a constant, independent of h.

Numerical Results

In this section we provide one dimensional numerical results for the scheme discussed above. The first and second test cases examine the coupled method's ability to handle high gradient regions, while the third test problem examines the order of convergence of the method. The LDG method based on $\mathcal{P}^1$ Legendre polynomials and the conforming Galerkin finite element method with linear basis functions were implemented on elements of equal size. Time discretization is by a second order accurate TVD Runge-Kutta method [11] with a sufficiently small time step so that error in time is negligible compared to spatial errors.

In the LDG method, we implemented a stability post-processing or slope-limiting procedure at each step of the calculation to prevent spurious oscillations. In each cell Ω_e, the linear approximation on this cell can be written as

$$C = C_e + \delta C_e (x - x_e),$$

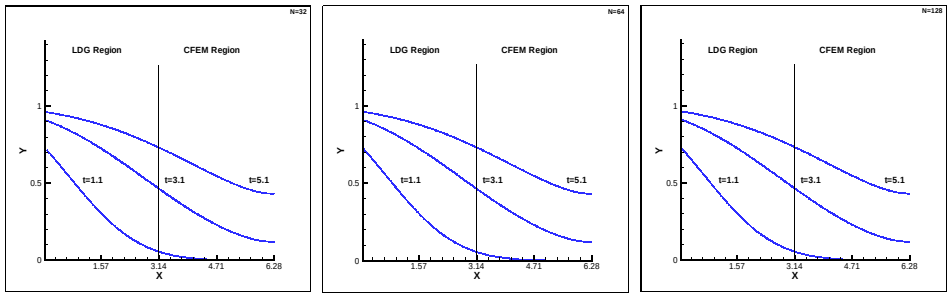

(a) 32 elements (b) 64 elements (c) 128 elements

Figure 1: Coupled approximate solution to convection diffusion test case 1.

where C_e and δC_e are determined from the variational form (29)-(32), and x_e is the midpoint of Ω_e. We then compare the slope δC_e to forward and backward difference approximations to the slope in each cell. That is, we compute,

$$|\bar{\delta C_e}| = \begin{cases} 0, & \text{if } (\delta^- C_e) * (\delta^+ C_e) < 0, \\ \min(|\delta C_e|, |\delta^- C_e|, |\delta^+ C_e|), & \text{otherwise,} \end{cases}$$

where $\delta^- C_e$ and $\delta^+ C_e$ are forward and backward differences of the cell averages. The sign of $\bar{\delta C_e}$ is chosen based on which quantity gives the minimum slope; $\bar{\delta C_e}$ then replaces δC_e above.

Test case 1

We first consider the problem

$$\begin{aligned} \partial_t c + u\partial_x c - D\partial_{xx} c &= 0, \quad 0 < x < 2\pi, \quad t > 0 \\ c(x,0) &= 0 \\ (uc - Dc_x)(0,t) &= u. \end{aligned}$$

We implemented the LDG method between $[0,\pi]$ and the CFE method between $[\pi, 2\pi]$ with the interface occuring at $x = \pi$. Figures 1 (a)-(c) show the coupled approximate solution, on meshes of 32, 64 and 128 equally spaced elements, with $u = 1.0$ and $D = 1.0$, at three points in time. These figures illustrate the ability of the method to propagate a solution smoothly through the interface. In each of these figures and the ones below, we have plotted the value of the solution at the midpoint of each element in the LDG region, and the value of the solution at each node in the CFE region.

Next we consider a convection dominated case with $u = 1.0$ and $D = .001$. Here we would expect a continuous Galerkin solution to be oscillatory, at least on coarse meshes. In Figures 2 (a)-(f), we compare approximate solutions for the coupled method and for the continuous Galerkin method, respectively, at five different times, for meshes of 32, 64 and 128 elements. As expected, the CFE solution is oscillatory for the coarser meshes, but gives a good solution on the finer mesh. The coupled method is also somewhat oscillatory in the CFE region for the coarser mesh, but gives good solutions on the two finer meshes. In particular, by using the LDG method in the first part of the domain, we are able to propagate the sharp front into the domain without oscillation. Once the solution is "smoothed" by the diffusion in the problem, the CFE method can then be used to further propagate the solution.

Since the LDG method involves more degrees of freedom than the CFE method, it is of interest to see how close we can move the interface location to the inflow boundary, before we start to see oscillatory behavior in the CFE region. Thus, we ran several experiments where we varied the location of the interface point. For example, for a mesh of 64 elements, with interface points at $\pi/2$ and $\pi/4$, the solution exhibited very little oscillation. However, as indicated in Figure 3, oscillations do begin to appear in the solution when the interface is at $\pi/8$. The solution here looks very similar to the CFE solution in Figure 1 (d). Thus, to avoid oscillatory behavior, one should propagate the solution sufficiently far into the domain using the LDG method, before letting the CFE method take over.

Test case 2

Here we consider the same problem as above, with the initial condition

$$c(x,0) = \begin{cases} 1, & 0 < x < .5 \\ 0, & \text{otherwise} \end{cases}$$

and inflow boundary condition $(uc - Dc_x)(0,t) = 0$. We again take $u = 1$ and $D = 0.001$. Thus, this problem describes the propagation of a square initial pulse, which slowly smooths out with time. In Figure 4, we compare the coupled LDG/CFE solution with interface at $x = \pi$ with a CFE solution, for 64, 128 and 256 elements. The CFE solution in this case overshoots and undershoots on all three meshes, though on the final mesh, the oscillations disappear as the solution propagates. The coupled LDG/CFE solution remains stable for all three meshes, but does exhibit slightly more numerical diffusion than the CFE solution.

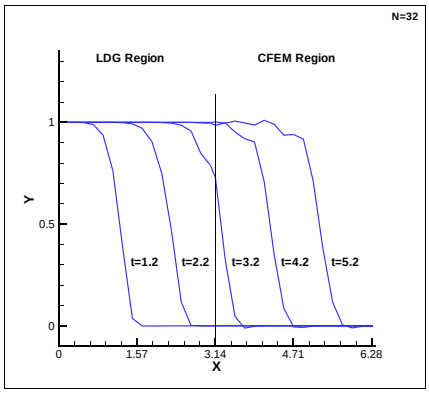

(a) Coupled N=32

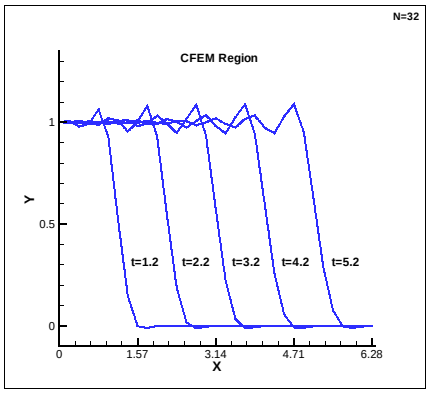

(b) Continuous N=32

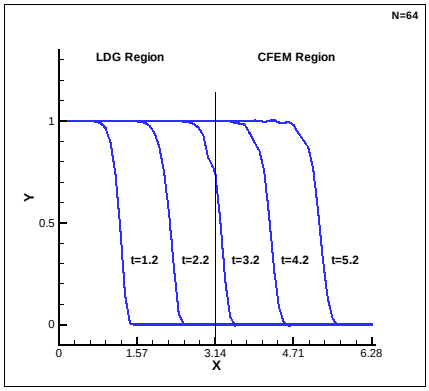

(c) Coupled N=64

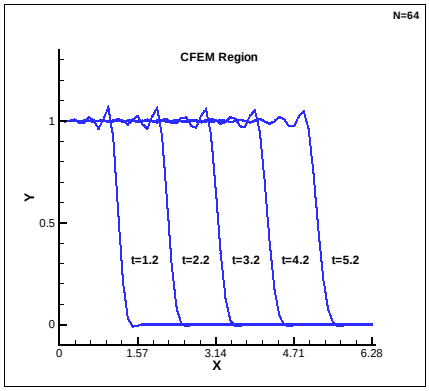

(d) Continuous N=64

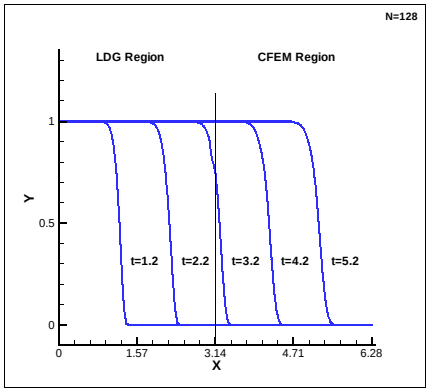

(e) Coupled N=128

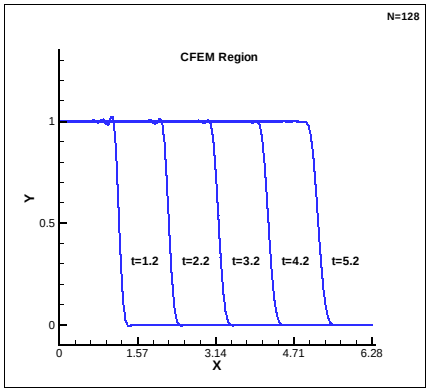

(f) Continuous N=128

Figure 2: Coupled and continuous approximate solutions to convection dominated test case 1.

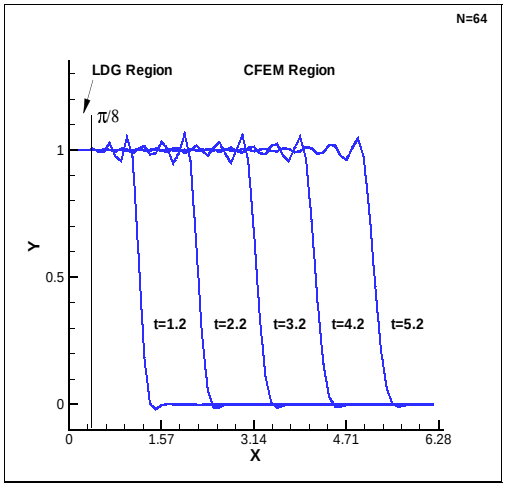

Figure 3: LDG/CFE solution with interface location at $\pi/8$.

Test case 3

Finally, we consider a smooth test problem:

$$\begin{aligned} \partial_t c + u\partial_x c - D\partial_{xx} c &= 0 \qquad && (0,T)\times(0,2\pi), \\ c(x,0) &= \sin(x) && \text{on } (0,2\pi), \end{aligned}$$

where various choices of u and D, and impose boundary conditions such that the exact solution is

$$c(x,t) = e^{-Dt} sin(x - u\,t). \tag{33}$$

The errors and convergence rates for variants of this problem are contained in Tables 1 through 4. At time T=1.0, we measured the L^2 error in $[0,2\pi]$ composed of an LDG region in $[0,\pi]$ and a CFE region in $[\pi,2\pi]$. In each of the test cases presented, "optimal" order ($\mathcal{O}(h^{p+1})$, in this case $p=1$) accuracy was observed, which is better than what we have proved above. Recall however, that our proof is valid for any space dimension, and does not rely on the positivity of D. For positive D, we have derived an improved convergence rate of order $k+1/2$ in $L^2(L^2)$ if certain penalty terms are included in the formulation [14]. We have not included these terms in the method presented here. Moreover, in one space dimension, an optimal order convergence rate (in both h and p) for the LDG method applied to convection-diffusion equations, has been proven by Castillo *et al* [6]. Their estimate assumes only a nonnegative diffusion coefficient D, but depends on a particular choice of the numerical fluxes between elements, and also on the use of a special projection of the true solution as a comparison function.

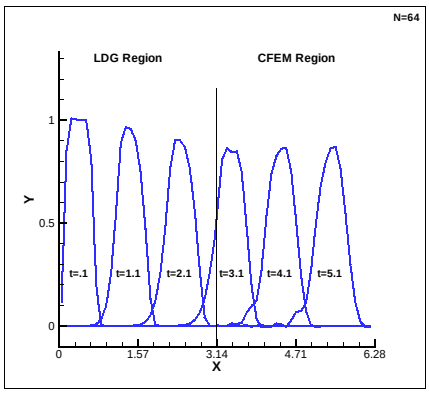

(a) Coupled N=64

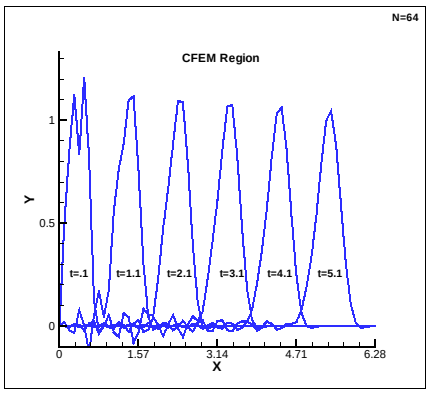

(b) Continuous N=64

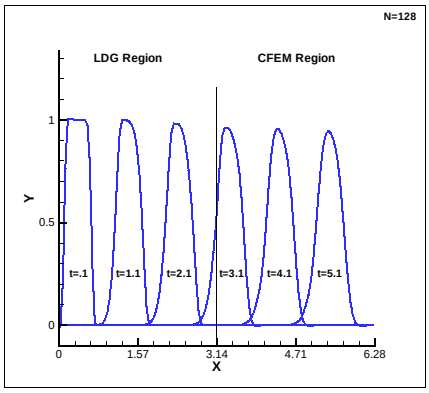

(c) Coupled N=128

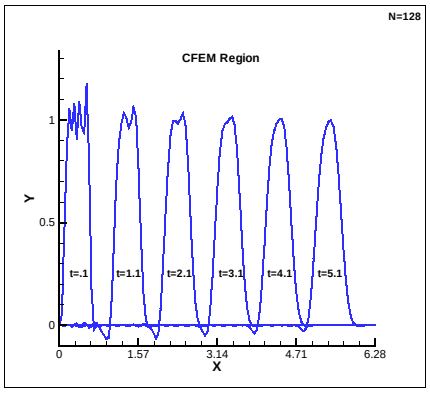

(d) Continuous N=128

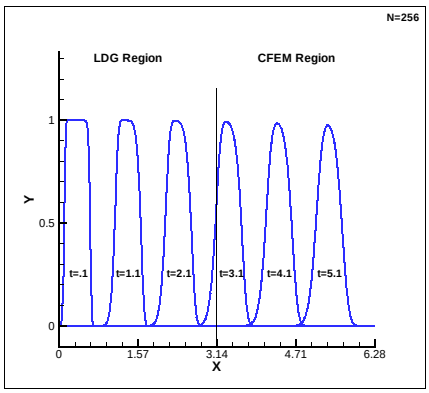

(e) Coupled N=256

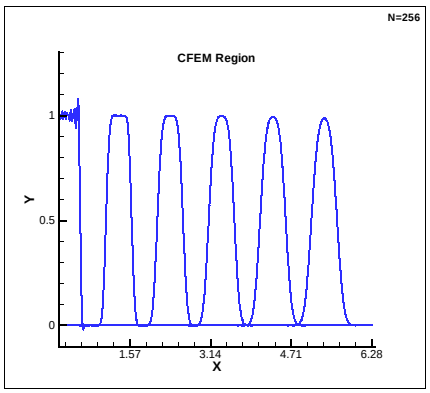

(f) Continuous N=256

Figure 4: Coupled and continuous approximate solutions to test case 2.

Table 1. The convection equation.

$u = 1.0$ $D = 0.0$	N	L^2 *error*	*k=1*
	32	.005299	
	64	.001322	2.00
	128	.000328	2.01
	256	.000080	2.04

Table 2. The heat equation.

$u = 0.0$ $D = 1.0$	N	L^2 *error*	*k=1*
	32	.004227	
	64	.001054	2.00
	128	.000263	2.00
	256	.000066	2.00

Table 3. The convection dominated equation.

$u = 1.0$ $D = 0.01$	N	L^2 *error*	*k=1*
	32	.005076	
	64	.001251	2.02
	128	.000309	2.02
	256	.000075	2.04

Table 4. The convection diffusion equation.

$u = 1.0$ $D = 1.0$	N	L^2 *error*	*k=1*
	32	.004152	
	64	.001049	1.99
	128	.000264	1.99
	256	.000066	2.00

Conclusions

A coupled discontinuous/continuous Galerkin method has been formulated for transport problems such as those arising in environmental quality modeling. Numerical results demonstrate the accuracy of the method and the ability to propagate sharp fronts.

Acknowledgment

This research was supported by NSF grants DMS-9873326 and DMS-9805491, and by the DoD High Performance Computing Modernization Program U.S. Army Engineer Research and Development Center (ERDC) Major Shared Resource Center through Programming Environment and Training (PET), supported by Contract Number: DAHC 94-96-C0002, Computer Sciences Corporation.

References

[1] V. Aizinger and C. Dawson, *Discontinuous Galerkin methods for two-dimensional flow and transport in shallow water*. to appear in Advances in Water Resources.

[2] V. Aizinger, C. Dawson, B. Cockburn, and P. Castillo, *Local discontinuous Galerkin methods for contaminant transport*, Advances in Water Resources, 24 (2000), pp. 73–87.

[3] P. Alotto, A. Bertoni, I. Perugia, and D. Schötzau, *Discontinuous finite element methods for the simulation of rotating electrical machines*, in Proceedings of 9th International IGTE Symposium on Numerical Field Calculation in Electrical Engineering, 2000.

[4] F. Bassi and S. Rebay, *A high-order accurate discontinuous finite element method for the numerical solution of the compressible Navier-Stokes equations*, J. Comput. Phys., 131 (1997), pp. 267–279.

[5] P. Castillo, B. Cockburn, I. Perugia, and D. Schotzau, *An a priori error analysis of the local discontinuous Galerkin method for elliptic problems.* to appear.

[6] P. Castillo, B. Cockburn, D. Schötzau, and C. Schwab, *An optimal a priori error estimate for the hp-version of the local discontinuous Galerkin method for convection-diffusion problems.* Math. Comp., to appear.

[7] B. Cockburn and C. Dawson, *Some extensions of the local discontinuous Galerkin method for convection-diffusion equations in multidimensions*, in The Proceedings of the Conference on the Mathematics of Finite Elements and Applications: MAFELAP X, J. R. Whiteman, ed., Elsevier, 2000, pp. 225–238.

[8] B. Cockburn, G. Kanschat, I. Perugia, and D. Schötzau, *Superconvergence of the local discontinuous Galerkin method for elliptic problems on Cartesian grids.* submitted.

[9] B. Cockburn, G. Kanschat, D. Schötzau, and C. Schwab, *Local discontinuous Galerkin methods for the Stokes system.* submitted.

[10] B. Cockburn, G. Karniadakis, and C.-W. Shu, *The development of discontinuous Galerkin methods*, in First International Symposium on Discontinuous Galerkin Methods, B. Cockburn, G. E. Karniadakis, and C.-W. Shu, eds., Springer-Verlag, 2000, pp. 5–50.

[11] B. Cockburn and C. W. Shu, *TVB Runge-Kutta local projection discontinuous Galerkin finite element method for scalar conservations laws II: General framework*, Math. Comp., 52 (1989), pp. 411–435.

[12] ——, *The local discontinuous Galerkin method for time dependent convection-diffusion systems*, SIAM J. Numer. Anal., 35 (1998), pp. 2440–2463.

[13] C. Dawson and J. Proft, *Coupling of continuous and discontinuous Galerkin methods for transport problems.* to appear.

[14] ——, *A priori error estimates for interior penalty versions of the local discontinuous Galerkin method applied to transport equations.* to appear in Numerical Methods for Partial Differential Equations.

[15] I. Perugia and D. Schötzau, *The coupling of local discontinuous Galerkin and conforming finite element methods.* submitted.